Highly reproducible perovskite solar cells via controlling the morphologies of the perovskite thin films by the solution-processed two-step method

RAHAQ, Yaqub, MOUSSA, Magdi, WANG, Heming and HASSAN, Aseel <http://orcid.org/0000-0002-7891-8087>

Published version

RAHAQ, Yaqub, MOUSSA, Magdi, WANG, Heming and HASSAN, Aseel (2018). Highly reproducible perovskite solar cells via controlling the morphologies of the perovskite thin films by the solution-processed two-step method. Journal of Materials Science: Materials in Electronics, 1-11.

Highly reproducible perovskite solar cells via controlling the morphologies of the perovskite thin films by the solution-processed two-step method

Yaqub Rahaq, Magdi Moussa, Abubaker Mohammad, Heming Wang, Aseel Hassan*

Materials & Engineering Research Institute, Sheffield Hallam University, City Campus, Howard Street, Sheffield, S1 1WB

*Corresponding author: aseel50.hassan@gmail.com

Abstract

Organic-inorganic halide perovskites are one of the most attractive materials for the next generation solar cells. The PCE has rapidly increased to more than 22% using different configurations and techniques and further developments are predicted. However, perovskite solar cells suffer from fabrication reproducibility mainly due to difficulty in controlling the morphology of the perovskite films themselves. In this paper we present a low temperature solution-processed two-step deposition method to fabricate $CH_3NH_3PbI_3$ perovskites. This method offers a simple route with great potential in fabricating reproducible perovskite solar cells. In the present work, we demonstrate that the morphology of the perovskite thin films is highly determined by the concentration of Methylammonium iodide (MAI) as well as the reaction time between MAI and PbI_2. High-performance solar cells have been reproducibly achieved with a highest PCE of 15.01% for PCBM-based planar heterojunction solar cells.

Key words: Halide perovskite; Solar cell; Films' morphology; Solution-processing, PCBM-based PHJ solar cell

1. Introduction

Organometallic halide perovskites have received significant interests in the last few years due to their superior optical and electrical properties. They demonstrated highly efficient capability of converting light into electricity with low-cost precursors and inexpensive solution-processed methods in fabricating the solar cells [1-7]. Power conversion efficiency (PCE) of perovskite solar cells has considerably soared from 3.8% in 2009 [8] to the certified efficiency of 22.7% in 2018 [9]. Studied perovskites solar cells were based on two types of typical device architectures, one type is based on TiO_2 [10-15] films and the other is based on phenyl-C61-butyric acid methyl ester (PCBM) planar heterojunction (PHJ) [16-20]. In order to achieve solar cells with high PCE, controlling the morphology of the perovskite thin films is one of the major challenges. In the published literature, perovskite films were produced by various methods, which include vacuum thermal deposition and solution-processed deposition by either one-step or two-step methods. Using the latter method, high-quality perovskite films were obtained utilising both approaches, with solar cells achieving high PCE. On the other hand, the major obstacle to the thermal evaporation method is ascribed to the high-cost of vacuum systems as well as its complicated processes. Furthermore, in order to control the morphology of the perovskite thin films in the one-step solution-processing method, two main routes were utilised; i) by adding additives into the precursor solution of the perovskites, and ii) by employing the so-called solvent engineering technology [21]. Nevertheless, it was found that uniform morphologies are difficult to be re-produced in the one-step method owing to their uncontrollable crystallisation rate during the fabrication process [22]. Therefore, the two-step method has been widely adopted as an efficient technique to control the morphology of the perovskite layer for both TiO_2-based and the PCBM-based perovskite solar cells. This is mainly ascribed to the ability to selectively

controlling the concentration in one of the precursors, and therefore controlling their reaction and crystallisation rates. For the TiO_2-based perovskite solar cells, different techniques were applied to control the morphologies including vapor-assisted solution-processing [23], halide sources mixing method [24], low-temperature gas-solid crystallisation processes [25], solution chemistry engineering [26], anti-solvent vapour-assisted crystallisation processes [27], and two-step ultrasonic spray deposition method [28]. Those methods however are complicated and may be expensive in some cases, although high-performance solar cells were obtained utilising one or another of the above highlighted methods. Furthermore, the TiO_2 layer has to be sintered at temperatures around 500°C [2], adding further difficulty to the processing of reliable TiO_2-based solar cells. Alternatively, the two-step fabrication method for the PCBM-based perovskite solar cells demonstrates a low-temperature processing route with favourable benefits as well as increased control of the perovskite films' morphologies. Different strategies have been used to control the crystallisation and to improve the morphologies of perovskite thin films in the PCBM-based perovskite solar cells. Shen et.al have employed the two-step annealing process to fabricate $CH_3NH_3PbI_3$ (assisted by doping with $PbCl_2$) perovskites thin films [29]. They found that thermal annealing has improved the surface coverage as well as the crystallisation of the perovskite films. PCE of 9.1% was achieved for solar cells based on this fabrication approach [29]. Haung et al claimed that the application of solvent annealing in the fabrication of perovskite films is an efficient technique to enhance the crystallinity of the perovskites, achieving 1 μm grain size of perovskites. The DMF was thought to promote grain growth due to the high solubility of both PbI_2 and MAI in DMF where the latter provide wet environment for the precursor ions and molecules to diffuse longer distance than in the case of all-solid annealing. Solar cells produced using such perovskite films have achieved PCE of 15.6% [30]. Chen and co-worker have used layer-by-layer technique to control the morphology of the perovskite film

[31]. $PbCl_2$ thin film was deposited by thermal evaporation, followed by dipping the film into a solution of CH_3NH_3I/IPA for several times to form a uniform perovskite layer [31]. Both solvent annealing and thermal annealing were shown to play a key role in controlling the crystal growth of the perovskites towards improvement of its morphology in the two-step method. However, various other factors can significantly affect the solvent annealing process, such as type and vapour pressure of solvents, process surrounding, and thermal annealing conditions (annealing temperature, duration and ramping level) [32]. Furthermore, reaction time between the pre-coated metal halide and MAI layer after being dipped into the solution of MAI requires an accurate control [23].

In this paper, we present a simple route to control the morphology of our perovskite films by the two-step deposition method used for the fabrication of PCBM-based PHJ solar cells. Through wide investigation of alternating the MAI concentration and its reaction time with the pre-deposited PbI_2 film, high-performance perovskite films were reproducibly obtained, resulting in perovskite solar cell structure with PCE of 15%. This technique has led to controlling the growth of perovskite crystals resulting in more compact film structure without pin holes and therefore leading to enhanced PCE of the perovskite film-based solar cell. Morphology and crystallinity of our perovskite films were extensively studied using SEM and XRD measurements.

2. Experimental

2.1 Preparation of materials

MAI was synthesised in ambient atmosphere at room temperature via the chemical reaction of 27 ml methylamine solution (CH_3NH_2, 40 wt% in methanol, TCI) with 30 ml of hydriodic acid (HI 57 wt.% in water, Aldrich) in a round-bottomed flask kept at 0 °C in an ice bath for 2 h. The methylamine solution was added first into the round-bottomed flask and then HI was

added drop-wise during stirring. White precipitate of MAI was collected after the mixture in the solution was transformed into a rotary evaporator and heated at 50°C for 1 h. The white precipitate was washed three times with diethyl ether and finally dried in vacuum for 24 h. PbI_2 solution was prepared by dissolving 1 mole PbI_2 in 1 ml DMF solvent and stirred at 70 °C. 20 µl of DIO was then added into the solution to promote the dissolution of PbI_2. The PbI_2 solution became clear after continuous overnight stirring at 70 ^oC. Thereafter, 0.5, 0.8, 1.0, 1.2 wt% MAI solution were separately produced by adding different amounts of MAI in 2-propanol and stirred for 1 h at 70°C. The PCBM solution was prepared by dissolving 30 mg of PCBM in 1 ml of chlorobenzene. 2 mg of bathocuproine (BCP) plus 20 µl acetic acid was dissolved in 1 ml of methanol to form the BCP solution.

2.2 Fabrication of solar cells

In the current study perovskite solar cells architecture comprises thin films of ITO/PEDOT:PSS/$CH_3NH_3PbI_3$/PCBM/BCP/Au, respectively; a flow chart illustrating the fabrication process is shown in Figure 1. ITO-coated glass substrates (ITO thickness is 100 nm) with sizes of ~ 20 x 25 mm were cleaned with soap and water followed by washing in deionised (DI) water. The substrates were blown dry in N_2 gas before they were separately cleaned ultrasonically in acetone and 2-propanol and finally blown dry again by N_2. The cleaned ITO substrates were spin-coated by PEDOT:PSS solution at spin speed of 3000 rpm followed by heating at 140 °C for 10 min. Thin films of PbI_2 were deposited on top of the PEDOT:PSS film by spin-coating at 5000 rpm using the high-purity supersaturated hot solution and then annealed at 70 °C for 8 min on a hot plate. MAI solution with different concentrations was added by drop casting on top of the PbI_2 thin film and left to react chemically with PbI_2 for various periods of time. The reactants were finally spin-casted at a rotation speed of 4000 rpm, and the obtained films were heated treated at 100 ^oC for 2 h. PCBM films were deposited by spin-coating method at 2000 rpm from PCBM solution on

top of the formed perovskite thin film, followed by heat treatment at 100 °C for 30 min. Electron transport layers of BCP of about 10 nm in thickness were spin-coated on top of the BCPM films followed by the deposition of Au films of about 100 nm as the top electrode using vacuum sputtering method.

2.3 Characterisation of solar cells

Current density as a function of applied voltage (J-V) of the PV devices fabricated in section 2.2 were measured under simulated AM 1.5G irradiation (100 mW/cm^2) using keithley 2401 source meter; the measurements were carried out under ambient environment. A Schott KG5 colour-filtered Si diode (Hamamatsu S1133) was utilised to calibrate the light intensity of the solar light simulator before J-V measurement were carried out. An aperture of aluminium mask was applied on the PV devices to obtain an active area of 0.04 cm² and to prevent any contribution from externally fallen light on the devices. X-ray diffraction (XRD) measurements of the perovskite layers were performed using Philips X'PERT MPD with operational parameters of 40 kV and 40 mA. Optical properties of the films were analysed using Varian 50 Scan UV–Vis Spectrophotometer. Scanning electron microscopy (SEM) was used to investigate morphology of the perovskite films using FEI-nova nanosem 200 SEM..

3. Results and discussion

3.1 MAI concentration effects on the perovskite crystal growth

Different concentrations of MAI in the range 0.5-1.2 wt% were separately utilised to apply onto the pre-coated PbI_2 thin films and allowing different reaction times (20 and 60 sec), followed by thermal annealing of the obtained perovskite films at 100°C for 2 hour.

A processing model to describe the formation of the perovskite thin film with different concentrations of the MAI solutions (0.5, 0.8, 1.0 and 1.2 wt%) is schematically presented in

Figure 2. When the MAI solution reached to the pre-coated PbI_2 crystals, nucleation of an intermediate phase of perovskites only happened at those areas where the MAI concentration must be greater than a threshold concentration (Ck); lower concentrations of MAI than Ck is not expected to result in such crystal growth. A specific reaction time between MAI and PbI_2 allows the growth of an intermediate phase of perovskite. This intermediate phase is then transformed into full perovskite phase after the film is thermally annealed at 100^oC. When the lower concentration of 0.5 or 0.8 wt% of MAI solution were applied onto the pre-formed PbI_2 film (as shown in Figure 2) only a small perturbation in the MAI concentration has led to some areas with locally high concentration of MAI, which resulted in the formation of a sporadically distributed intermediate phase of $CH_3NH_3PbI_3$. Only when the concentration of MAI increased to 1.0 wt%, the distributed amount of MAI on the whole surface area of the PbI_2 film was maintained at a concentration above Ck, and thus a gradually controlled crystal growth happened. Thin films with a uniform intermediate perovskite phase were formed after the reaction was maintained for about one minute. Longer growth (reaction) time and higher concentration of MAI will lead to the lift-off of the intermediate perovskite phase from the substrate, which will then lead to reduction in the thickness of the final perovskite film by the following spin-coating process.

Scanning electron microscopy (SEM) was used to study the morphology of the perovskite films and the results are shown in Figure 3. When the lowest concentration of 0.5 wt% MAI was added onto the pre-coated PbI_2 film, the size of the perovskite crystals increased from ~ 0.7 μm for the 20 sec reaction time to ~ 1.0 μm for the 60 sec reaction time, as seen in Figure 3a and 3b. When comparing Figure 3a with Figure 3b, the slightly dissolved PbI_2 film was observed except the sporadically distributed perovskite crystals, which did not cover the whole surface. In other words, most of the PbI_2 crystals were only slightly dissolved by the MAI solution. The low MAI concentration has led to low nucleation density and thus low

crystallisation of the perovskites. Further increase in the reaction time between MAI and PbI_2 did not make any contribution to the enhancement of the nucleation density on the surface of the PbI_2 film. Interestingly, with the increase of the MAI concentration to 0.8 wt%, we noticed that crystallisation occurred with an increased surface coverage on the PbI_2 thin film as indicated in Figure 3c and 3d. However, the size of the perovskite crystals decreased to ~ 0.4 μm regardless of how long the reaction time was. With a further increase of the MAI concentration to 1.0 wt%, the coverage of the perovskite surface reached full coverage of the original PbI_2 surface, meaning that all PbI_2 crystals have reacted with MAI to form perovskites as shown in Figure 3e and 3f. Again, we observed that the size of perovskites continued to decrease to about 0.2 μm.

Nevertheless, when the concentration of the MAI solution further increased to 1.2 wt %, pore defects among the smaller nano-sized perovskite crystals were revealed in Figure 3g and 3h. As shown in Figure 3, the size of the perovskite crystals in the film did not change with extending reaction time from 20 sec to 60 sec when using high concentrations of 0.8, 1 and 1.2 wt % of MAI solutions. These results confirm that the size of crystals in the perovskite film was determined in the initial reaction stage when the MAI solution came into contact with the pre-coated PbI_2.

SEM was also used to further study the morphology of the cross section of the perovskite films and the results are shown in Figure 4. Figure 4a shows a cross section SEM image of the perovskite film fabricated by the 0.8 wt% MAI solution, where the corresponding thickness of the perovskite film was ~ 400 nm. The image shows that the nano-sized polycrystals of $CH_3NH_3PbI_3$ did not connect together as was also shown in Figure 3c and 3d, where considerable residual PbI_2 phases have existed in the film. As demonstrated in Figure 3e and 3f, interconnected $CH_3NH_3PbI_3$ crystals without any residual PbI_2 phases were only formed after applying 1.0 wt% MAI solution onto the pre-coated PbI_2 film. The thickness of

the perovskite film was ~ 200 nm as demonstrated in Figure 4b. A further increase in the MAI solution concentration to 1.2 wt% has led to the formation of pore defects among the smaller nano-sized perovskite crystals as revealed in Figure 3g and 3h. The thickness of the perovskite film has exhibited a significant decrease to ~120 nm as demonstrated by the cross section image in Figure 4c.

3.2 Effect of MAI concentration on light absorption and crystal structure of perovskite films

Light absorption by the formed perovskite films was examined to study the impact of the MAI concentrations on the optical properties of the perovskite films. All perovskite films with different MAI concentrations show absorption onset at ~ 780 nm as shown in Figure 5, which could conform to a band gap value of ~1.52 eV for the perovskites. The perovskite film produced by the low concentration of 0.8 wt% MAI exhibited the highest thickness as shown in Figure 4a, and thus the highest light absorption. On the other hand, the perovskite film obtained by the highest MAI concentration of 1.2 wt% resulted in the lowest thickness which is associated with a significant decrease in the absorption intensity as demonstrated in Figure 5. The perovskite thin film produced from the 1.0 wt% MAI solution showed an excellent light absorption between the perovskite films obtained by 0.8 wt% and 1.2 wt% MAI solutions.

X-ray diffraction measurements (XRD) were used to characterise the crystalline structure of the perovskites films produced with different MAI concentrations and the results are presented in Figure 6. All perovskite films were prepared under the same condition on glass slides with exactly the same size. Diffraction peaks that belong to $CH_3NH_3PbI_3$ polycrystals are indicated by "■" while the main peaks assigned to the residual PbI_2 phase are illustrated by "●". The XRD pattern of the film produced from the lowest MAI concentration (0.5 wt%) reveals different peak positions at 2Θ of 8.2°, 12.8°, 14.2°, 20.09°, 23.8°, 28.4°, 31.9°, 40.7°,

42.6° and 52°. Most peaks belong to the perovskite structure except the peaks at 8.2° and 12.8° are due to the residual PbI_2 phase. According to Qiu and co-workers, the measured peaks at 2Θ of 14.2°, 20.09°, 23.8°, 28.4°, 31.9°, 40.7° and 42.6° may correspond to the (110), (112), (211), (220), (310), (224) and (314) crystal faces of the tetragonal perovskite [33]. The high intensity of the two peaks at 2Θ of 8.2° and 12.8° indicates the considerable presence of residual PbI_2 phases in the sample. Increasing the MAI concentration to 0.8 wt% led to more perovskite phases in the film as shown in Figure 6, where the two peaks assigned to the residual PbI_2 phase have reduced significantly. When the MAI concentration reached 1.0 wt%, only peaks assigned to the perovskite phase can be observed in the XRD pattern, suggesting that PbI_2 phase has completely changed to perovskites via reaction. For the films produced with a higher concentration of MAI of 1.2 wt%, the main diffraction peak at 2Θ of 14.2° for the perovskite phase has decreased in intensity due to the reduction in film thickness.

3.3 Solar cells performance of perovskites from different MAI concentrations

It has been shown earlier that the concentration of the MAI solution and reaction time between MAI and PbI_2 are crucial to obtain high-quality perovskite thin films for solar cell applications. It can therefore be expected that such high quality films would play a key role in achieving reproducible solar cell characteristics and thus high PCE. Main perovskite phase was achieved when one minute reaction time was utilized between MAI and PbI_2. Therefore, different concentrations of MAI solution were taken to fabricate perovskite thin films with one minute reaction time with PbI_2 in order to study the properties of the thus produced solar cells.

The quality of the perovskite thin films has played a key role in determining the PCE of solar cells. The concentration of the MAI solution and reaction time between MAI and PbI_2 are crucial to obtain high-quality perovskite thin films. We have found that reproducible solar

cell characteristics were achieved when one minute reaction time was utilised. Therefore, different concentrations of the MAI solution and one minute reaction time were taken to fabricate perovskite thin films for our solar cells to compare with their PCEs. Figure 7 shows J-V characteristics of solar cells produced with different MAI concentrations. Among all measured characteristics, the best performance was achieved with solar cells produced using perovskite film made with 1.0 wt.% MAI solution deposited onto the pre-coated PbI_2 thin film. A summary of performance of all PV devices is listed in Table 1. It is shown that solar cells made with 1.0 wt% MAI concentration have demonstrated typical performance with PCE of 15.01%, short circuit current of 23.8 mA/cm², and fill factor of 0.70. Such high performance solar cells were achieved as a result of uniform, homogeneous, and connected perovskite thin films. Solar cells produced with 1.2 wt% MAI solution exhibited a reduction in their performance. A low PCE of 6.76% can be ascribed to the low current density of 14.7 mA/cm^2 and low FF of 0.5 measured for such devices. The smaller thickness of the perovskite film obtained from using such MAI concentration may be considered as the main reason for the low device performance. Furthermore, solar cells produced with perovskite film from the 0.8 wt% MAI solution have demonstrated the poorest PCE of 4.19%, which is the consequence of low current density of 11.4 mA/cm^2 and very poor FF of 0.38. The high proportion of the residual PbI_2 phase in the perovskite thin film may be considered as the main culprit for the poor performance. The other reason for such poor performance may be ascribed to the poor surface coverage of the perovskite film leading to formation of pin holes and thus short circuit current. All studied perovskite solar cells produced with different MAI concentrations have demonstrated high open-circuit voltage above 0.9 V.

Figure 8 shows J-V characteristics of perovskit solar cells made with 1.0 wt% MAI solution measured both in the dark and under illumination of 100 mW cm^{-2}. This particular device has demonstrated very good PV characteristics with PCE of 15.01%. Figure 9 presents a

statistical distribution of performance of 135 solar cells fabricated from the 1.0 wt% MAI solution, showing excellent reproducibility of perovskite solar cells with high performance.

The influence of hysteresis on our perovskite solar cells is also investigated in the current work. Figure 10 shows J-V measurements of perovskit solar cells made with 1.0 wt% MAI solution scanned in forward and reverse bias directions, where the phenomenon of hysteresis is considered as one of main concerns in the stability of perovskite-based solar cells [34]. Our solar cells exhibited convergent performance in PCE under both forward and reverse scan directions, suggesting almost negligible hysteresis effect. This is credited to the reduction in the density of defects due to the controlled morphologies of our perovskite films by the two-step fabrication method [34]. The decent interface between the perovskite layer and the electron or hole transport layers can be another reason for the mitigation of the hysteresis effect in the perovskite solar cells [35].

4. Conclusion

The low-temperature two-step fabrication method was used to produce the high quality $CH_3NH_3PbI_3$ thin films for PHJ solar cells. It was found that concentration of the MAI solution and reaction time between MAI and PbI_2 have a significant impact on the morphologies and crystal growth of the perovskite thin films. Highly reproducible perovskite thin films were fabricated for solar cells application when 1.0 wt% MAI solution was applied to preformed PbI_2 films. Among 110 solar cells from the best perovskite films made with the 1.0 wt.% MAI solution and one minute reaction time about one third have exhibited an average performance with PCE of 13.63 % while the highest achieved PCE was of 15.01%.

Acknowledgements

The authors would like to acknowledge the facility support by Sheffield Hallam University technical staff and Becker Industrial Coating Ltd.

References

[1] Y. Hou, H. Zhang, W. Chen, S. Chen, C. O. R. Quiroz, H. Azimi, A. Osvet, G. J. Matt, E. Zeira, J. Seuring, N. K. Busies, W. Lövenich and C. J. Brabec, Inverted, Environmentally Stable Perovskite Solar Cell with a Novel Low‐Cost and Water‐Free PEDOT Hole‐Extraction Layer. Adv. Energy Mater. 5, 1500543 (2015)

[2] C. Bi, Y. Shao, Y. Yuan, Z. Xiao, C. Wang, Y. Gao and J. Huang, Understanding the formation and evolution of interdiffusion grown organolead halide perovskite thin films by thermal annealing. J Mater Chem A. 2, 18508-18514 (2014)

[3] K. G. Lim, H. B. Kim, J. Jeong, H. Kim, J. Y. Kim and T. W. Lee, Boosting the Power Conversion Efficiency of Perovskite Solar Cells Using Self‐Organized Polymeric Hole Extraction Layers with High Work Function. Adv. Mater. 26, 6461-6466 (2014)

[4] H. Zhang, H. Azimi, Y. Hou, T. Ameri, T. Przybilla, E. Spiecker, M. Kraft, U. Scherf, and C. J. Brabec, Improved high-efficiency perovskite planar heterojunction solar cells via incorporation of a polyelectrolyte interlayer. Chem. Mater. 26, 5190-5193 (2014)

[5] G. Xing, N. Mathews, S. Sun, S. Lim, Y. Lam, M. Grätzel and S. Mhaisalkar, Long-range balanced electron-and hole-transport lengths in organic-inorganic CH3NH3PbI3. Science. 342, 344-347 (2013)

[6] S. A. Kulkarni,T. Baikie, P. P. Boix, N. Yantara, N. Mathews and S. G. Mhaisalkar, Band-gap tuning of lead halide perovskites using a sequential deposition process. J Mater Chem A. 2, 9221–9225 (2014)

[7] J. H. Noh, S. H. Im, J. H. Heo, T. N. Mandal and S. I. Seok, Chemical management for colorful, efficient, and stable inorganic–organic hybrid nanostructured solar cells. Nano Lett. 13, 1764-1769 (2013)

[8] A. Kojima, K. Teshima, Y. Shirai and T. Miyasaka, Organometal halide perovskites as visible-light sensitizers for photovoltaic cells. J. Am. Chem. Soc. 131, 6050–6051 (2009)

[9] M. Tavakoli, D. Bi, L. Pan, A. Hagfeldt, S. Zakeeruddin and M. Grätzel, Adamantanes Enhance the Photovoltaic Performance and Operational Stability of Perovskite Solar Cells by Effective Mitigation of Interfacial Defect States. Adv. Energy Mater. 1800275 (2018)

[10] S. Karuppuchamy, G. Murugadoss, K. Ramachandran, V. Saxena, R. Thangamuthu, Inorganic based hole transport materials for perovskite solar cells. J. Mater. Sci. Mater. Electron. 29(10), 8847–8853 (2018)

[11] K. Wojciechowski, M. Saliba, T. Leijtens, A. Abate and H. J. Snaith, Sub-150 C processed meso-superstructured perovskite solar cells with enhanced efficiency. ENERG ENVIRON SCI. 7, 1142-1147 (2014)

[12] J. T. Wang, J. M. Ball, E. M. Barea, A. Abate, J. A. A. Webber and J. Huang, M. Saliba, I. Mora-Sero, J. Bisquert, H. J. Snaith, R.J. Nicholas, Low-temperature processed electron collection layers of graphene/TiO2 nanocomposites in thin film perovskite solar cells. Nano Lett. 14, 724-730 (2013)

[13] P. Qin, A. L. Domanski, A. K. Chandiran, R. Berger, H. J. u. Butt, M. I. Dar, T. Moehl, N. Tetreault, P. Gao, S. Ahmad, M. K. Nazeeruddin and M. Gratzel, Yttrium-substituted nanocrystalline TiO 2 photoanodes for perovskite based heterojunction solar cells. Nanoscale. 6, 1508-1514 (2014)

[14] J. W. Lee, S. H. Lee, H. S. Ko, J. Kwon, J. H. Park, S. M. Kang, N. Ahn, M. Choi, J. K. Kim and N. G. Park, Opto-electronic properties of TiO 2 nanohelices with embedded HC (NH 2) 2 PbI 3 perovskite solar cells. J Mater Chem A. 3, 9179-9186 (2015)

[15] N. G. Park, Organometal perovskite light absorbers toward a 20% efficiency low-cost solid-state mesoscopic solar cell. J. Phys. Chem. Lett. 4, 2423-2429 (2013)

[16] J. H. Kim, C. C. Chueh, S. T. Williams and A. K. Y. Jen, Room-temperature, solution-processable organic electron extraction layer for high-performance planar heterojunction perovskite solar cells. nanoscale.7, 17343-17349 (2015)

[17] S. Ryu, J. Seo, S. S. Shin, Y. C. Kim, N. J. Jeon, J. H. Noha and S. I. Seok. Fabrication of metal-oxide-free CH 3 NH 3 PbI 3 perovskite solar cells processed at low temperature. J Mater Chem A. 3, 3271-3275 (2015)

[18] C. H. Chiang, Z. L. Tseng and C. G. Wu, Planar heterojunction perovskite/PC 71 BM solar cells with enhanced open-circuit voltage via a (2/1)-step spin-coating process. J Mater Chem A . 2, 15897-15903 (2014)

[19] J. Duan, Q. Xiong, H. Wang, J. Zhang and J. Hu, ZnO nanostructures for efficient perovskite solar cells. J. Mater. Sci.: Mater. Electron. 28, 60 (2017)

[20] J. Seo, S. Park, Y. C. Kim, N. J. Jeon, J. H. Noh, S. C. Yoon and S. I. Seok, Benefits of very thin PCBM and LiF layers for solution-processed p–i–n perovskite solar cells. ENERG ENVIRON SCI. 7, 2642-2646 (2014)

[21] L. Zheng, D. Zhang, Y. Ma, Z. Lu, Z. Chen, S. Wang, L. Xiao, Q. Gong, Morphology control of the perovskite films for efficient solar cells. Dalt Trans. 44, 10582–10593 (2015)

[22] S. Shi, Y. Li, X. Li, H. Wang, Advancements in all-solid-state hybrid solar cells based on organometal halide perovskites. Mater Horizons. 2, 378-405 (2015)

[23] Chen Q, Zhou H, Hong Z, S. Luo, H. S. Duan, H. H. Wang, Y. Liu, G. Li, Y. Yang, Planar heterojunction perovskite solar cells via vapor assisted solution process. J Am Chem Soc. 136, 622-625 (2013)

[24] Jiang M, Wu J, Lan F, Q. Tao, D. Gao, G. Li, Enhancing the performance of planar organo-lead halide perovskite solar cells by using a mixed halide source. J Mater Chem A. 3, 963–967 (2015)

[25] Hao F, C. C. Stoumpos, Z. Liu, R. P. Chang, M. G. Kanatzidis, Controllable perovskite crystallization at a gas–solid interface for hole conductor-free solar cells with steady power conversion efficiency over 10%. J Am Chem Soc. 136, 16411–16419 (2014)

[26] Zhao Y, Zhu K, Solution Chemistry Engineering toward High-Efficiency Perovskite Solar Cells. J Phys Chem Lett 5, 4175–4186 (2014)

[27] D. Shi, V. Adinolfi, R. Comin, , M. Yuan, E. Alarousu, A. Buin, Y. Chen, S. Hoogland, A. Rothenberger, K. Katsiev, Y. Losovyj, Low trap-state density and long carrier diffusion in organolead trihalide perovskite single crystals. Science . 347, 519-522 (2015)

[28] Huang H, Shi J, L. Zhu, D. Li, Y. Luo, Q. Meng, Two-step ultrasonic spray deposition of CH3NH3PbI3 for efficient and large-area perovskite solar cell. Nano Energy. 27, 352-358 (2016)

[29] H. L. Hsu, C. P. Chen, J. Y. Chang, Y. Y. Yu, Y. K. Shen, Two-step thermal annealing improves the morphology of spin-coated films for highly efficient perovskite hybrid photovoltaics. Nanoscale. 6, 10281-10288 (2014)

[30] Z. Xiao, Q. Dong, C. Bi, Y. Shao, Y. Yuan, J. Huang, Solvent Annealing of Perovskite-Induced Crystal Growth for Photovoltaic-Device Efficiency Enhancement. Adv Mater. 26, 6503-6509 (2014)

[31] Y. Chen, T. Chen, L. Dai, Layer-by-Layer Growth of CH 3 NH 3 PbI 3− x Cl x for Highly Efficient Planar Heterojunction Perovskite Solar Cells. Adv Mater. 27, 1053-1059 (2015)

[32] Y. Zhao, K. Zhu, Solution Chemistry Engineering toward High-Efficiency Perovskite Solar Cells. J Phys Chem Lett. 5, 4175-4186 (2014)

[33] J. Qiu, Y. Qiu, K. Yan. M. Zhong, C. Mu, H. Yan, S. Yang, All-solid-state hybrid solar cells based on a new organometal halide perovskite sensitizer and one-dimensional TiO 2 nanowire arrays. Nanoscale 5, 3245 (2013)

[34] H. J. Snaith, A. Abate, J. M. Ball, G. E. Eperon, T. Leijtens, N. K. Noel, S. D. Stranks, J. T. W. Wang, K. Wojciechowski, W. Zhang, Anomalous hysteresis in perovskite solar cells. J. Phys. Chem. Lett. 5, 1511–1515 (2014)

[35] G. E. Eperon, V. M. Burlakov, A. Goriely , H. J. Snaith. Neutral color semitransparent microstructured perovskite solar cells. ACS Nano. 8, 591–598 (2014).

Table 1 Device performance against varied concentrations of the MAI solution

Concentration of MAI (wt%)	**V_{oc} (V)**	**J_{sc} (mA/cm²)**	**FF**	**PCE (%)**
0.8	0.95	11.4	0.38	4.19
1	0.92	23.8	0.70	15.01
1.2	0.92	14.7	0.50	6.76

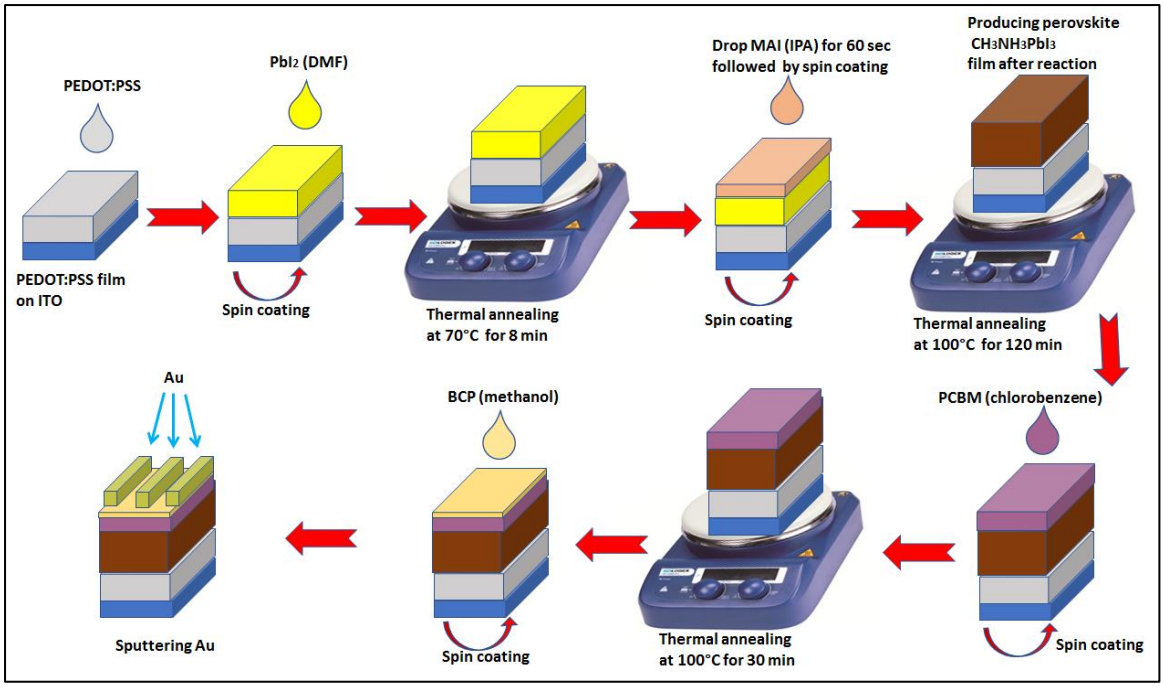

Figure 1: Fabrication process of perovskite solar cells (CH3NH3PbI3) using two-step static spin coating technique

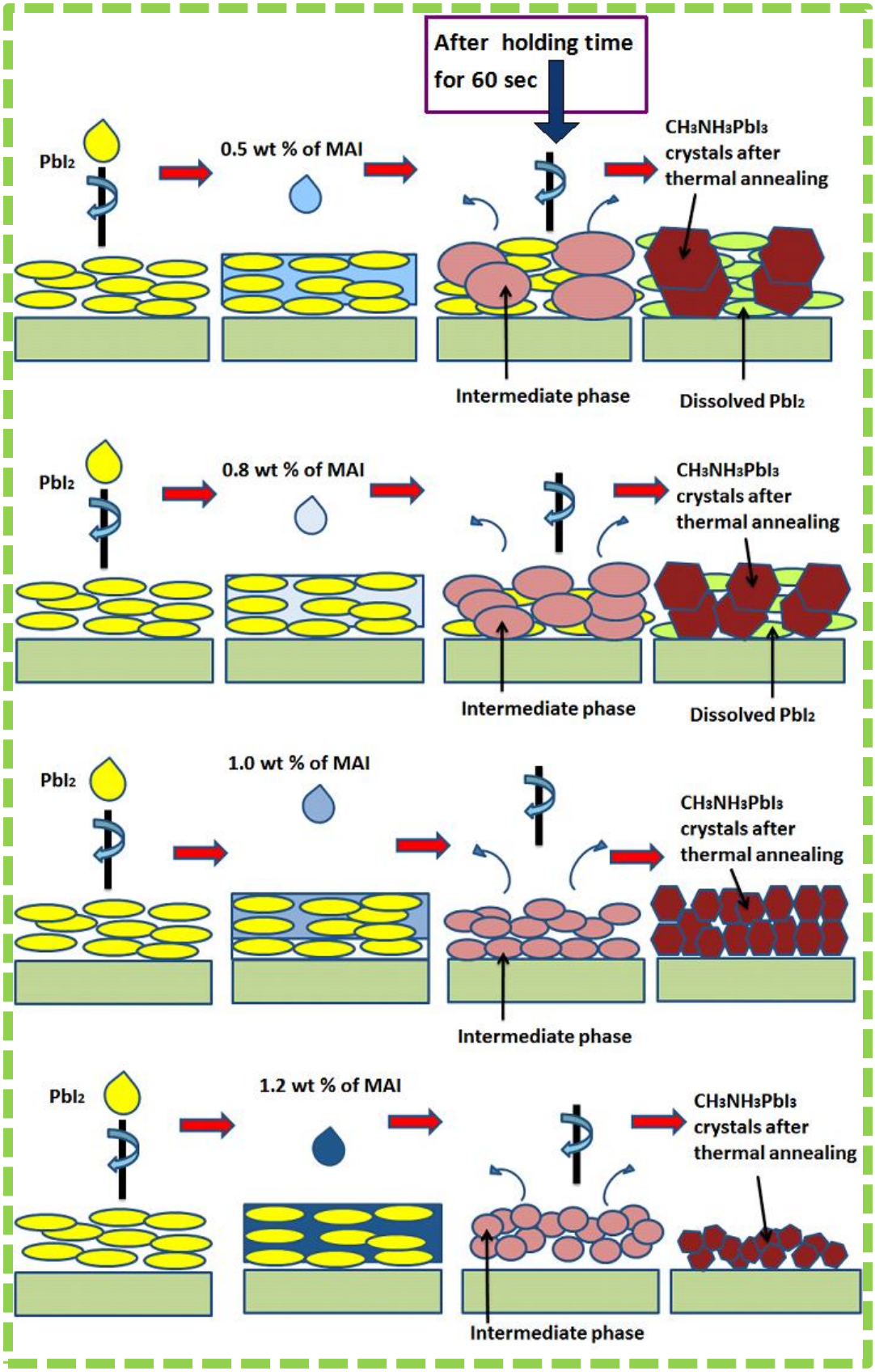

Figure 2: A schematic diagram of the processing model for the formation of perovskite thin films by different MAI concentrations.

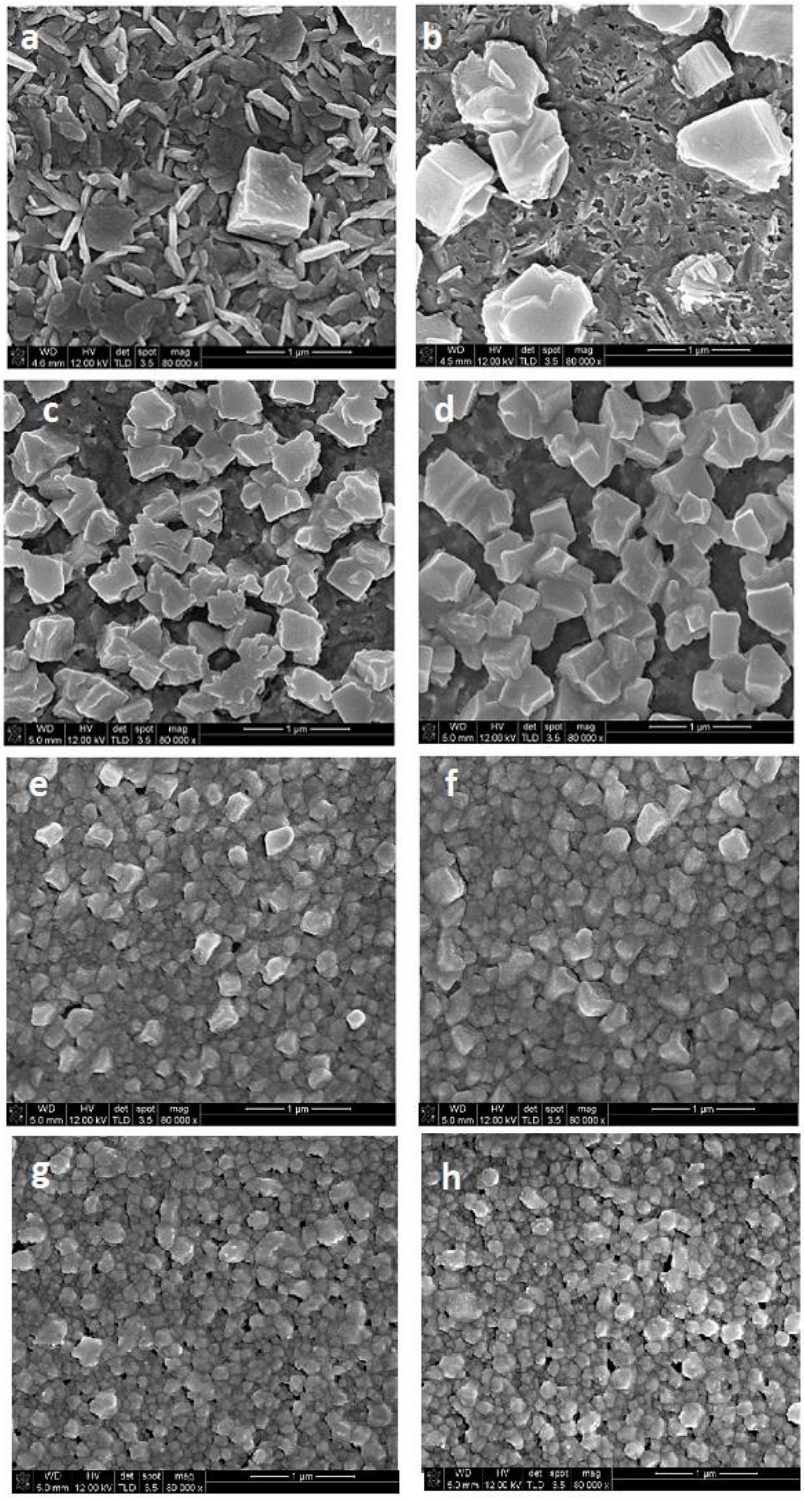

Figure 3: SEM images of the perovskite films with different MAI concentrations and 20 or 60 seconds reaction time, respectively: a) 0.5 wt%. 20 sec; b) 0.5 wt%. 60 sec; c) 0.8 wt%. 20 sec; d) 0.8 wt%. 60 sec; e) 1.0 wt%. 20 sec; f) 1.0 wt% 60 sec; g) 1.2 wt% 20 sec; h) 1.2 wt% 60 sec.

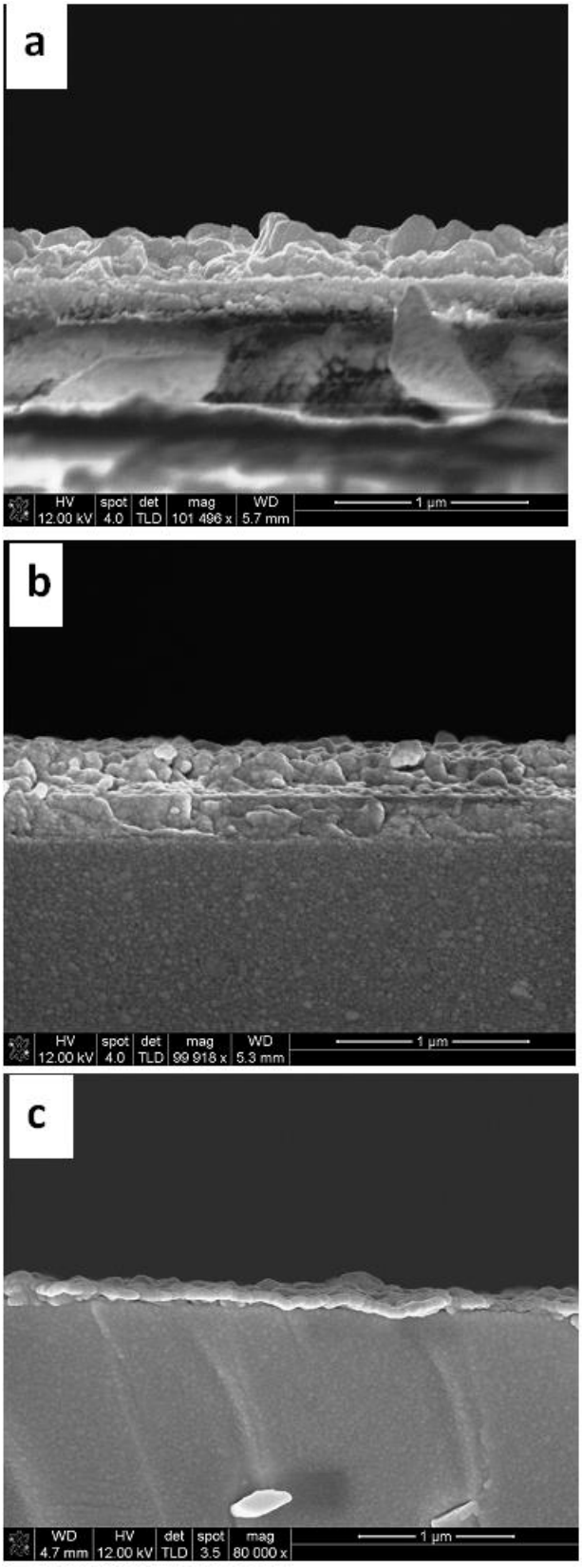

Figure 4: SEM cross section images of the perovskite films with different MAI concentrations: a) 0.8 wt. %; b) 1.0 wt. %; c) 1.2 wt. %.

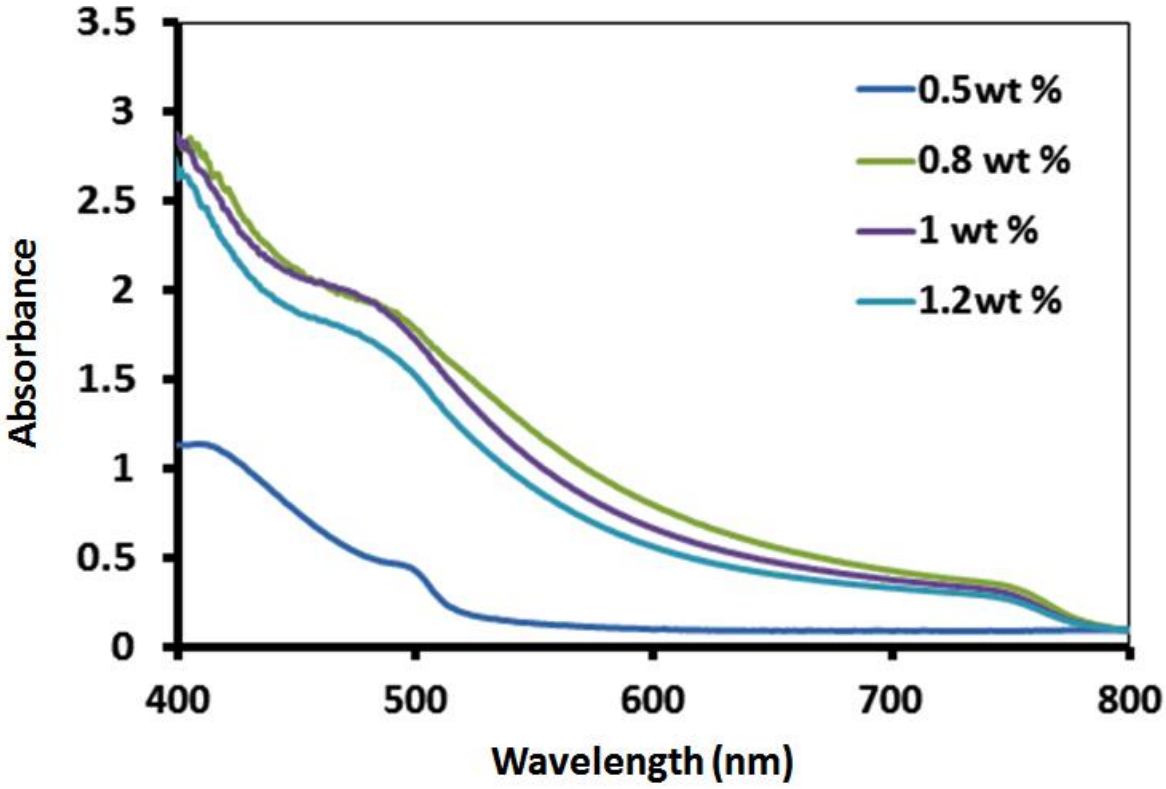

Figure 5: UV-Vis absorption spectra of $CH_3NH_3PbI_3$ films with different MAI concentrations and 60 sec reaction time.

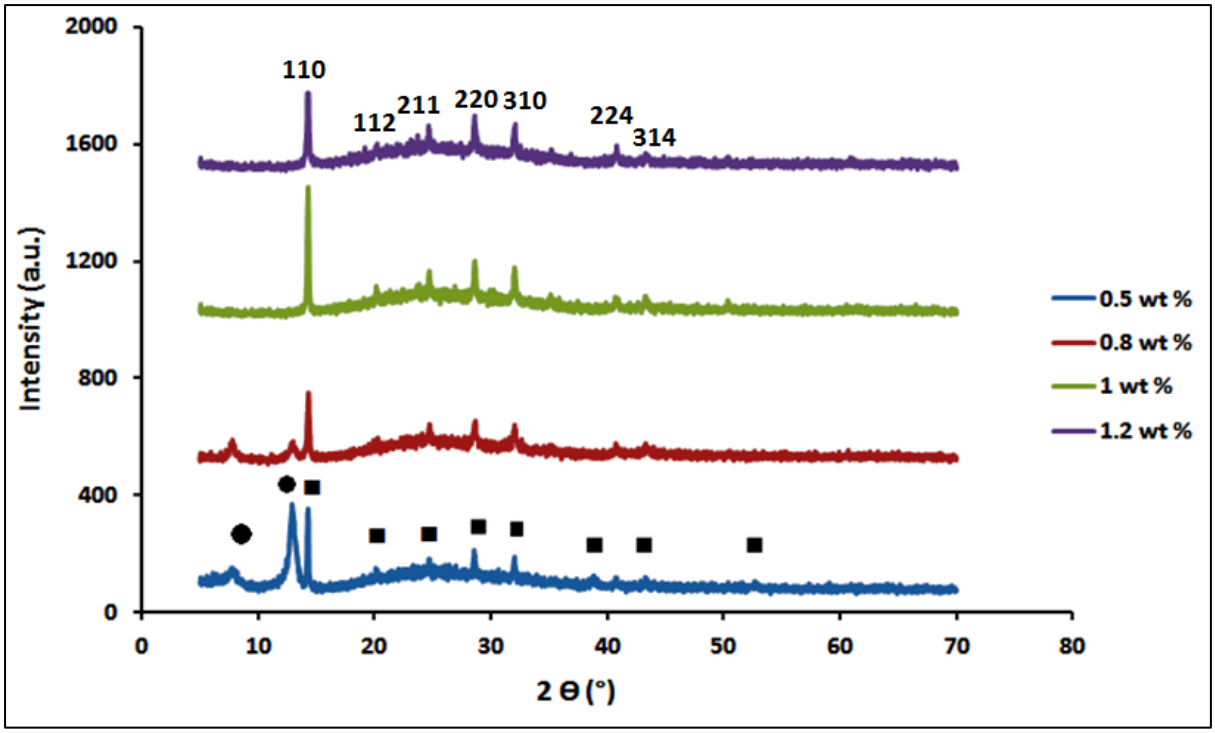

Figure 6: X-ray diffraction patterns of $CH_3NH_3PbI_3$ solar cells with different MAI concentrations and 60 sec reaction time.

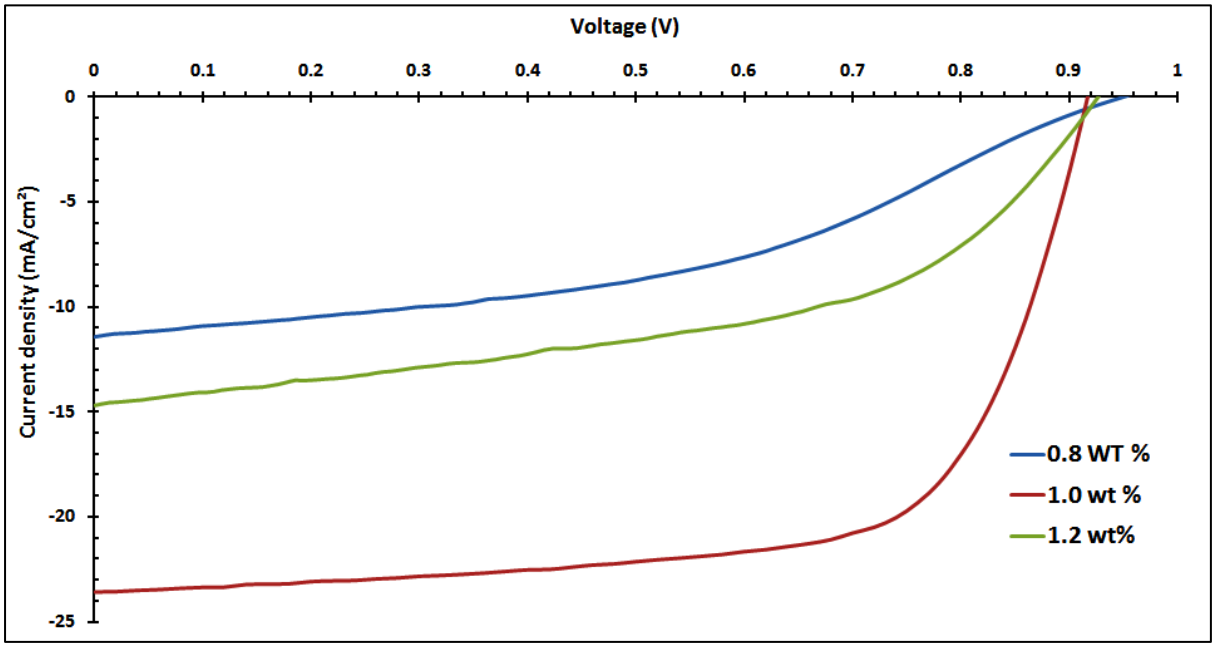

Figure 7: J-V performances of the perovskite solar cells with different MAI concentrations and 60 sec reaction time.

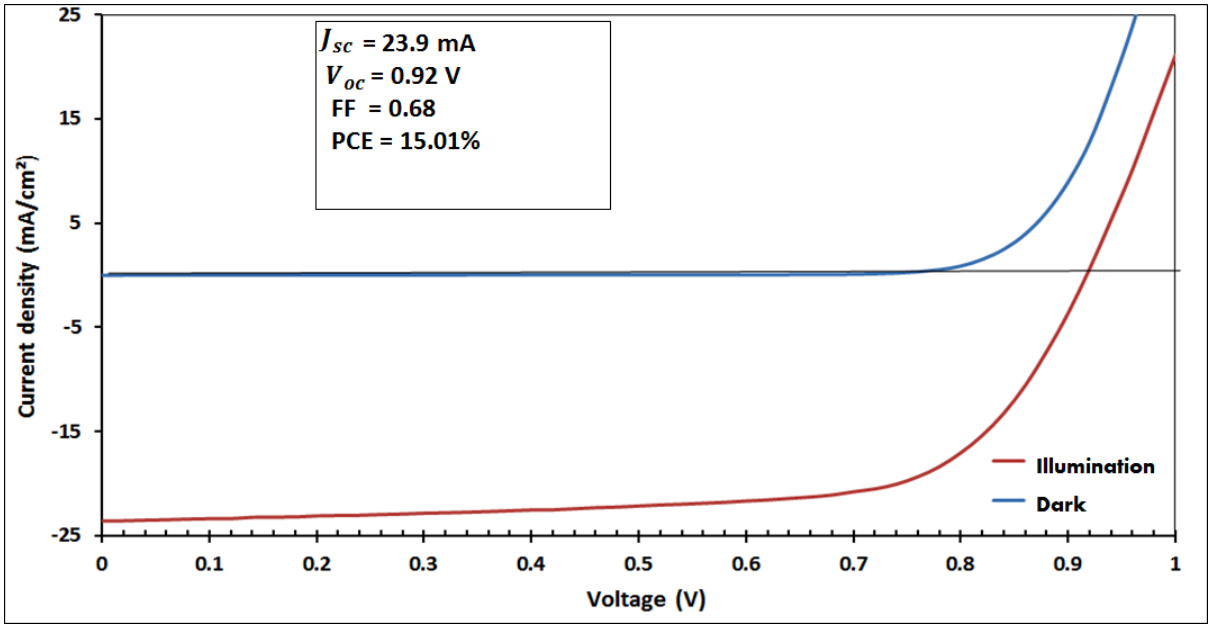

Figure 8: J-V performances for the best solar cell under illumination and dark conditions, respectively.

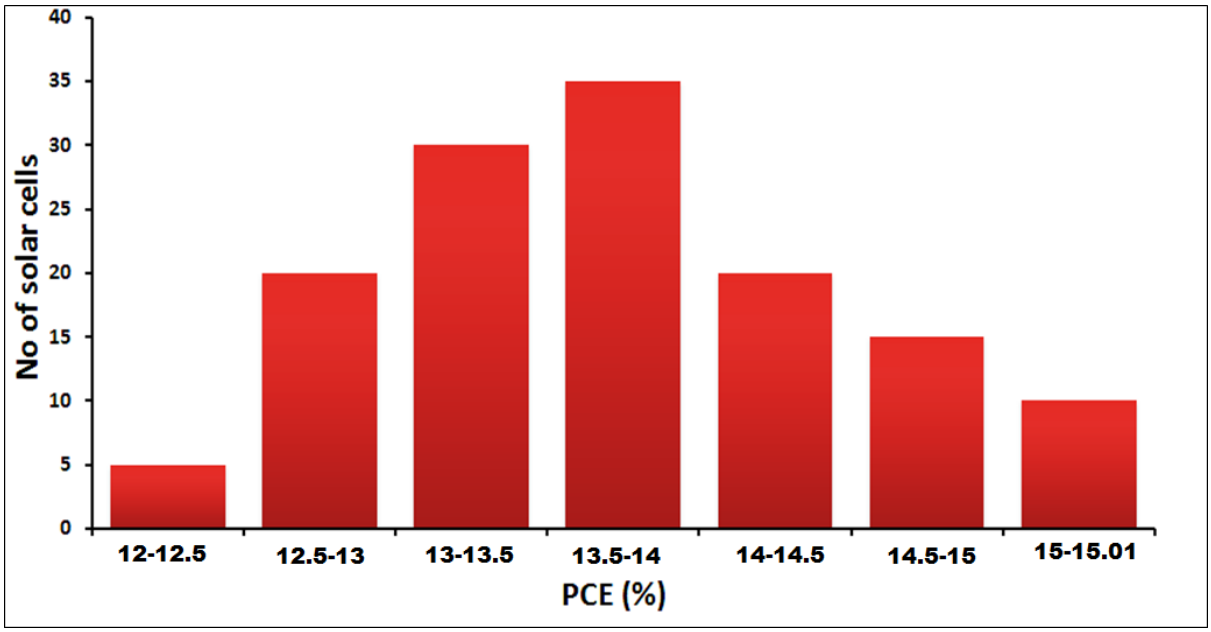

Figure 9: the performance distribution of 135 solar cells fabricated from the 1.0 wt% MAI solution

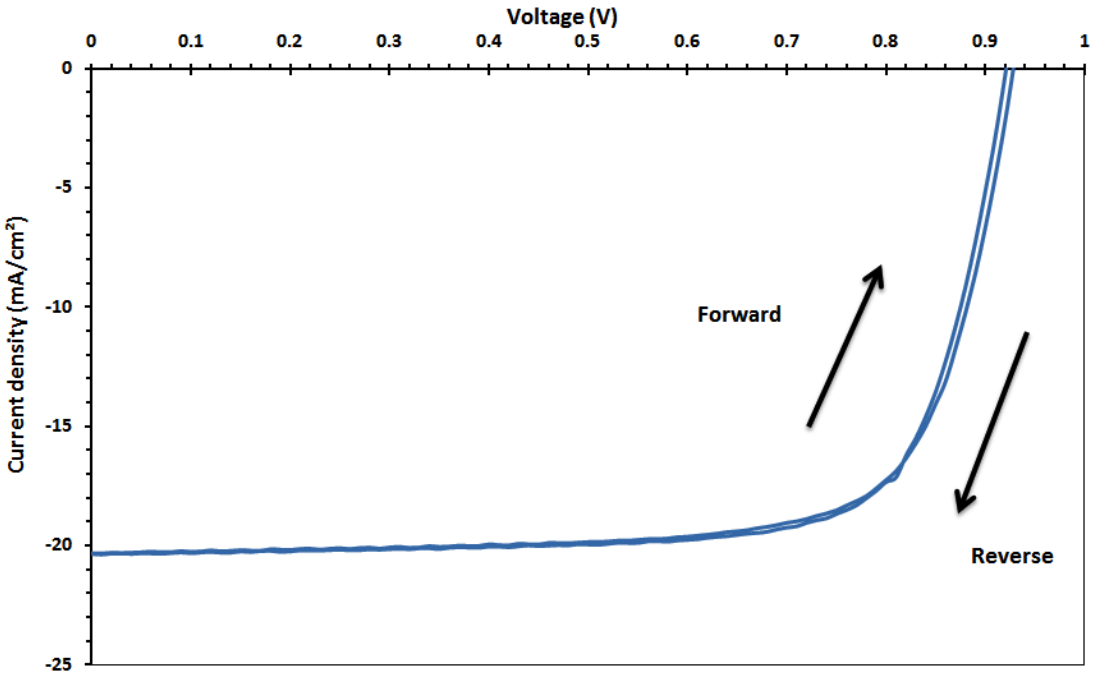

Figure 10: J-V curves under forward and reverse scan for the typical perovskite solar cells.